JSCE Journal of Earthquake Engineering

SEISMIC LOAD INPUTS AND RESPONSE ANALYSIS OF INELASTIC SDOF STRUCTURES IN SITES LACKING EARTHQUAKE DATA

A M ABBAS[1,2], Kazuo TAKAHASHI[3] and Shozo NAKAMURA[4]

[1]Lecturer, Department of Civil Engineering, Faculty of Engineering, Minia University, Minia 61111, Egypt
[2]Visiting Faculty, Department of Civil Engineering, Faculty of Engineering, Nagasaki University,
1-14 Bunkyo-machi, Nagasaki 852-8521, Japan, abbas@civil.nagasaki-u.ac.jp
[2]Professor, Department of Civil Engineering, Faculty of Engineering, Nagasaki University,
1-14 Bunkyo-machi, Nagasaki 852-8521, Japan, takahasi@civil.nagasaki-u.ac.jp
[3]Associate Professor, Department of Civil Engineering, Faculty of Engineering, Nagasaki University,
1-14 Bunkyo-machi, Nagasaki 852-8521, Japan, snakamura@civil.nagasaki-u.ac.jp

The modeling of earthquake loads as design inputs for inelastic sdof structures in sites lacking earthquake data is considered. The earthquake load is expanded as a linear summation of past recorded ground motions with unknown coefficients. The resulting nonlinear optimization problem is solved such that the structure inelastic deformation is maximized subject to a set of predefined constraints. The structure force-displacement relation is taken to possess an elastic-plastic behavior. Influences of yield strength and damping ratio on modeling earthquake inputs for inelastic structures and issues related to dissipated energy are explored. Numerical illustrations on modeling critical seismic load inputs for an elastic-plastic frame structure at a firm soil site are provided.

key words: *Earthquake loads, inelastic structures, ductility factor, dynamic response, nonlinear optimization*

1. INTRODUCTION

The problem of modeling earthquake ground motions as design inputs for engineering structures has received significant research attention worldwide. The present practice is to use the method of design response spectra, the time history analysis or the method of random vibration. On the other hand, the method of critical earthquake load modeling has been established, during the last three decades, as a counterpart to these methods. This method relies on the fact that, for many parts of the world, available data on strong earthquake ground motion is either inhomogeneous or insufficient. Given that each earthquake event brings out new surprises, it is thus of significant interest to develop robust specification for earthquake inputs to engineering structures. The recent December 2004 Asia earthquake of magnitude 9.0 is a remarkable example in this direction (PEER Center)[1)]. The huge energy generated by this earthquake beneath the Indian Ocean caused several tsunamis to spread out in all directions, affecting Sri Lanka, Southern India, and even the east coast of Africa. The massive waves washed over islands and crashed against coastlines in these countries. Tens of thousands of people were killed while millions became homeless.

Early works on modeling critical earthquake loads has been carried out by Drenick[2)], Shinozuka[3)] and Iyengar[4)]. An extensive overview of the development of this method is reported by Takewaki[5)], Abbas and Manohar[6)] and Abbas[7)]. This method can be developed within deterministic and/or probabilistic framework. In the deterministic approach the earthquake load is defined as an acceleration time history or in terms of response spectra. In the probabilistic approach the earthquake ground motion is modeled as a random process. Regardless of the framework adopted, critical earthquake loads depend upon the structure considered, the site soil conditions and the constraints imposed on the earthquake signal. In implementing this method, the earthquake load is taken to be known only partially. Subsequently, an inverse dynamic problem is solved to compute the unknown information on the seismic input, such that, a pre-selected damage variable of the structure is maximized. At the same time the computed load, termed as *critical* excitation, satisfies a set of constraints that impart known features of real earthquake ground motion. Since critical earthquake loads represent extreme load scenario, it is, thus, essential to consider the structure nonlinear behavior.

While the problem of modeling critical earthquake loads for linear structures is widely studied, the determination of critical earthquake excitations for nonlinear structures, however, has been studied to a very limited extent in the existing literature[5-7]. Iyengar[8] modeled critical earthquake loads for nonlinear Duffing oscillators by imposing a constraint on the input total energy. Drenick[9] extended his earlier study on linear structures to nonlinear structures using equivalent linearization. He showed that the critical excitation for a nonlinear system is again, except for a constant factor, the time reversed impulse response function of the linearized system. Philippacopoulos and Wang[10] developed critical inelastic response spectra using recorded ground accelerograms as basis functions in a series representation for the critical seismic excitation. Westermo[11] defined critical response in terms of input energy to the system and determined critical excitations for elastic-plastic and hysteretic single-degree-of-freedom (sdof) systems using calculus of variations. The critical loads for inelastic systems were not harmonic and at low frequencies the response is significantly larger than the harmonically excited response. A similar study to that reported by Westermo was carried out by Pirasteh et al.,[12]. These authors computed critical excitations for inelastic multi-story frame structures under deterministic earthquake inputs. The response variable adopted for maximization was chosen as the cumulative inelastic energy dissipation or sum of inter-story drifts. The objective functions, in this study, were evaluated using approximate methods to reduce the computational costs of the nonlinear dynamic response analysis of the optimization algorithm. Recently, Takewaki[13,14] developed critical random earthquake inputs for sdof and multi-degree-of-freedom (mdof) elastic-plastic systems. This author utilizes the method of statistical linearization to approximately evaluate the structure response. The variable of optimization in these two studies has been the sum of the response standard deviations of inter-storey drifts normalized to yield drifts. More recently, Abbas and Manohar[15] have developed a reliability-based framework for determining random critical earthquake loads for nonlinear structures. This study integrates methods of structural reliability analysis, response surface modeling and nonlinear programming in computing seismic inputs for structures having cubic force-displacement relations. The damage variable adopted in this study was the structure reliability index.

The present study treats the problem of modeling critical earthquake loads for inelastic structures. The earthquake acceleration is modeled as a deterministic time history which is expressed as a linear combinations in terms of a set of past recorded ground motions. Subsequently, the coefficients of the series representation are computed such that the structure inelastic response is maximized subject to a set of predefined constraints. Namely, an upper bound on the earthquake total energy and peak values of ground acceleration, velocity and displacement are considered. The structure force-displacement relation is taken to possess elastic-plastic behavior. The resulting nonlinear optimization problem is solved by using the sequential quadratic optimization method. Since, to the best of authors' knowledge, the influence of yield strength and damping ratio on modeling critical earthquake excitations has not been studied earlier the present study examines these aspects. Additionally, for sake of comparison, critical earthquake inputs for the elastic structure are also computed. Numerical illustrations on modeling critical earthquake loads for an elastic-plastic frame structure found at a firm soil site are provided.

2. INELASTIC SDOF STRUCTURES UNDER EARTHQUAKE LOAD

The equation of motion for the relative displacement *u(t)* of an inelastic sdof system subject to a single component of ground acceleration $\ddot{u}_g(t)$ (see figure 1(a)) is well known to be given by[16)]

$$m\ddot{u}(t) + c\dot{u}(t) + f_s(u,\dot{u}) = -m\ddot{u}_g(t) \qquad (1)$$

Here, *m, c* are mass and damping of sdof system and $f_s(u,\dot{u})$ is the spring restoring force. Figure 1(b) depicts the nature of $f_s(u,\dot{u})$ for nonlinear systems with elastic-plastic force-displacement characteristic. Herein, the restoring force is not only a function of the displacement response but depends on the velocity response as well. The above equation of motion may describe the dynamic analysis of a single-storey frame structure or a piping system under a uniform ground motion $\ddot{u}_g(t)$. It may be noted that, for systems governed by the above equation of motion, the force-deformation relation is no longer a single valued relation. Thus, for a displacement $u(t_i)$ at time t_i the spring force depends upon prior history of motion of the system and whether velocity response $\dot{u}(t_i)$ is increasing or decreasing. In the present study, damping is taken to be viscous, and, also, it is assumed that system starts from rest. Equation (1) can be recast as

$$\ddot{u}(t) + 2\zeta\omega\dot{u}(t) + \omega^2 u_y \bar{f}_s(u,\dot{u}) = -\ddot{u}_g(t) \qquad (2)$$

where, $\zeta = c/2\sqrt{km}$ is the damping ratio, $\omega = \sqrt{k/m}$ is the natural frequency for the linear system or for the elastic-plastic system undergoing small deformations (i.e. $u < u_y$) and u_y is the yield displacement. It may be recalled that, at larger amplitudes the natural vibration period is not defined for inelastic systems. The function $\bar{f}_s(u,\dot{u})$ may be defined as the spring restoring force in a dimensionless form. Referring to the above equation, it may be noted that for a given earthquake acceleration $\ddot{u}_g(t)$, the displacement response depends on the natural frequency ω, the damping ratio ζ and the yield displacement u_y (see figure 1(b)). Herein, $u_y = f_y/k$, where f_y is the yield strength and k is the initial stiffness. The dynamic analysis of inelastic structures governed by Equation (2) can be carried out by integrating this equation. Alternatively, response of these systems can be characterized in terms of the inelastic displacement response normalized to the yield displacement (known as the ductility factor). Defining this factor as $\mu(t) = u(t)/u_y(t)$ and substituting into Equation (2) one gets

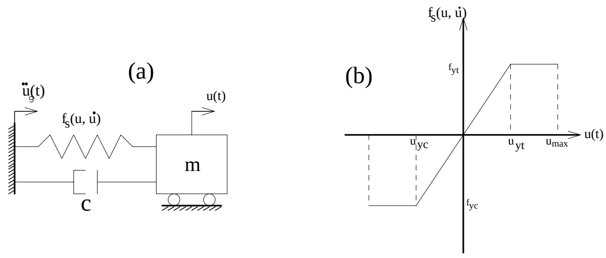

Figure 1. (a) Inelastic sdof system (b) Elastic-plastic behavior

$$\ddot{\mu}(t) + 2\zeta\omega\dot{\mu}(t) + \omega^2 \bar{f}_s(\mu,\dot{\mu}) = -\omega^2 \frac{\ddot{u}_g(t)}{a_y} \qquad (3)$$

It follows from this equation that the ductility factor for systems driven by a time-variant dynamical load is also a time-variant quantity. It may be observed that the expressions $\ddot{u}(t) = u_y\ddot{\mu}(t)$ and $\dot{u}(t) = u_y\dot{\mu}(t)$ were employed in deriving the above equation. The constant $a_y = f_y/m$ appearing in the right side of this equation may be interpreted as the acceleration of the mass necessary to produce the yield force f_y and $\bar{f}_s(\mu,\dot{\mu})$ is the force-deformation relation in dimensionless form. Furthermore, the acceleration ratio $\ddot{u}_g(t)/a_y$ is the ratio between the ground acceleration and a measure of the yield strength of the structure. For instance, Equation (3) implies that doubling the ground acceleration $\ddot{u}_g(t)$ will produce the same response $\mu(t)$ as if the yield strength had been halved. The response analysis of inelastic systems governed by the above equation of motion (or Equation (2)) is generally carried out using numerical integration techniques.

3. CRITICAL EARTHQUAKE LOADS FOR INELASTIC SDOF STRUCTURES

The ground acceleration $\ddot{u}_g(t)$ appearing in the right side of Equation (3) is taken to be known only partially. Specifically, the information available on the ground acceleration $\ddot{u}_g(t)$ is assumed to be limited to its total energy and peak values of ground acceleration, velocity and displacement. Accordingly, the problem of modeling critical earthquake excitations for elastic-plastic structures can be stated as computing $\ddot{u}_g(t)$ such that the structure inelastic response is maximized subject to the following set of constraints

$$[\int_0^\infty \ddot{u}_g^2(t)dt]^{1/2} \le E; \max_{0<t<\infty} |\ddot{u}_g(t)| \le M_1; \quad \max_{0<t<\infty} |\dot{u}_g(t)| \le M_2; \max_{0<t<\infty} |u_g(t)| \le M_3 \tag{4}$$

Herein, the quantities E, M_1, M_2 and M_3 represent upper bounds on the energy, peak acceleration, peak velocity and peak displacement of the input ground motion. To determine these quantities, it is assumed that a set of earthquake records denoted by $\ddot{v}_{gi}(t)$, $i=1, 2, ..., N_r$ are available for the site under consideration or from other sites which are geologically similar to the given site. The values of energy, peak values of acceleration, velocity and displacement are obtained for each of these records. The highest of these values across the ensemble of the records are taken to be the respective estimates of E, M_1, M_2 and M_3. The set of available records $\ddot{v}_{gi}(t)$ are further normalized so that the energy of each record is set to unity, and these normalized records are denoted by $\ddot{\bar{v}}_{gi}(t)$. As a first step to solve this optimization problem the ground acceleration $\ddot{u}_g(t)$ is expanded in terms of normalized past recorded accelerations as follows

$$\ddot{u}_g(t) = \sum_{i=1}^{N_r} a_i \ddot{\bar{v}}_{gi}(t) \tag{5}$$

Here, a_i, $i = 1, 2, ..., N_r$ is a set of N_r unknown constants, $\ddot{\bar{v}}_{gi}(t)$ is the ith normalized record and N_r is the number of available records. Mathematically, the problem of computing critical earthquake loads for inelastic sdof systems can be posed as computing the optimization variables a_i, $i = 1, 2, ..., N_r$, such that the structure inelastic response is maximized subject to the following constraints

$$\begin{aligned} &[\sum_{i=1}^{N_r}\sum_{j=1}^{N_r} a_i a_j \int_0^\infty \ddot{\bar{v}}_{gi}(t)\ddot{\bar{v}}_{gj}(t)dt]^{\frac{1}{2}} \le E; \\ &\max_{0<t<\infty} |\sum_{i=1}^{N_r} a_i \ddot{\bar{v}}_{gi}(t)| \le M_1; \\ &\max_{0<t<\infty} |\sum_{i=1}^{N_r} a_i \dot{\bar{v}}_{gi}(t)| \le M_2; \\ &\max_{0<t<\infty} |\sum_{i=1}^{N_r} a_i \bar{v}_{gi}(t)| \le M_3 \end{aligned} \tag{6}$$

This constitutes a constrained nonlinear optimization problem and is solved using the sequential quadratic programming method[17)]. An initial guess for the optimization variables a_i, $i = 1, 2, ..., N_r$, is supplied to the optimization program. Subsequently, the optimization routine performs a sensitivity analysis searching for new values for these variables. The optimization code converges to the optimal solution when the following criteria on the objective function and optimization variables are satisfied

$$|\mu_j - \mu_{j-1}| \le \ell_1; |a_{ij} - a_{ij-1}| \le \ell_2; i = 1,2,...,N_r \tag{7}$$

Herein, j represents the iteration number, a_{ij} is the ith optimization variable at the jth iteration and ℓ_1, ℓ_2 are the convergence limits. It may be emphasized that the structure inelastic response is determined by numerical integration of the equation of motion using the Newmark-β method. The details of the steps involved in the computation of optimal earthquake loads and the associated response can be summarized as follows:

1. Define the structure parameters m, c, k, the yield strength in tension and compression f_{yt}, f_{yc} and determine the parameter $a_y = f_{yt}/m$.
2. Set the initial conditions $\mu(0)$ and $\dot{\mu}(0)$ and compute the corresponding quantity $\ddot{\mu}(0)$ from the equilibrium of Equation (3). Herein, the initial conditions $u(0) = 0$ and $\dot{u}(0) = 0$ and the transformation $\mu(t) = u(t)/u_y$ are employed in determining $\mu(0)$ and $\dot{\mu}(0)$.
3. Select the time step Δt and calculate the constants of the Newmark-β method ($a_1 = \beta/\Delta t$, $a_2 = 2/\beta$, $a_3 = 1 - 1/4\beta$, $a_4 = 1/\beta\Delta t^2$).
4. Determine the initial yield ductility points $\mu_{yt} = u(t)|_{t=t_{yt}} / u_{yt}$ and $\mu_{yc} = u(t)|_{t=t_{yc}} / |u_{yc}|$. Here, t_{yt} and t_{yc} define the time points at which system starts to yield in tension and in compression, respectively.
5. For $t = t_j$ use the value of the parameter KEY to establish the elastic or plastic state of the structure based on the following criteria
   - KEY = 0 implies elastic behavior
   - KEY = 1 implies plastic behavior in tension
   - KEY = -1 implies plastic behavior in compression
6. Calculate the incremental effective force

$$\Delta F_j = \frac{-\omega^2}{a_y}\Delta\ddot{u}_{gj} + (a_1 + 2a_2\zeta\omega)\dot{\mu}_j + (a_2 - 2a_3\zeta\omega)\ddot{\mu}_j \tag{8}$$

7. Calculate the effective stiffness

$$K_j = \omega^2 k_p + a_1\zeta\omega + a_4 \tag{9}$$

Here, $k_p = k$ for elastic behavior (KEY = 0) and k_p = 0 for plastic behavior (KEY = 1 or -1).

8. Compute the incremental displacement

$$\Delta\mu_j = \frac{\Delta F_j}{K_j} \tag{10}$$

9. Solve for the incremental quantity

$$\Delta\dot{\mu}_j = 2a_1\Delta\mu_j - a_2\dot{\mu}_j + a_3\Delta t\ddot{\mu}_j \tag{11}$$

10. Calculate the quantities

$$\mu_{j+1} = \mu_j + \Delta\mu_j\ ;\ \dot{\mu}_{j+1} = \dot{\mu}_j + \Delta\dot{\mu}_j \tag{12}$$

11. Set the new value for the parameter KEY as follows

- When the system is behaving elastically at the beginning of the time step then KEY = 0 if $\mu_{yc} < \mu_j < \mu_{yt}$, KEY = -1 if $\mu_j > \mu_{yt}$ and KEY = -1 if $\mu_j < \mu_{yc}$.
- When the system is behaving plastically in tension at the beginning of the time step then KEY = 1 if $\dot{\mu}_j > 0$ and KEY = 0 if $\dot{\mu}_j < 0$.
- When the system is behaving plastically in compression at the beginning of the time step then KEY = -1 if $\dot{\mu}_j < 0$ and KEY = 0 if $\dot{\mu}_j > 0$.

12. Compute the incremental quantity

$$\ddot{\mu}_{j+1} = \frac{-\omega^2}{a_y}\ddot{u}_{gj+1}(t) - 2\zeta\omega\dot{\mu}_{j+1} - \omega^2\bar{f}_s(\mu_{j+1}, \mu_{j+1}) \tag{13}$$

Here, $\bar{f}_s(\mu_{j+1}, \dot{\mu}_{j+1})$ is given as $1-(\mu_j - \mu_{j+1})$ if KEY = 0, 1 if KEY = 1 and -1 if KEY = -1.

13. Repeat steps 5 to 12 for all discrete points of time (j = 1, 2, …, N_p, and Np is the number of discrete points of time)

14. The optimal normalized inelastic response is computed as $\mu(t_m) = \max\limits_{1\le j\le N_p} |\mu(t_j)|$. The corresponding set of optimization variables a_i, $i=1, 2, \ldots, N_r$ define the critical $\ddot{u}_g(t)$ (Equation 5) and associated critical inelastic response.

4. NUMERICAL RESULTS AND DISCUSSIONS

4.1 Structure considered

To illustrate the formulation developed in the preceding section, the determination of optimal earthquake excitations for an elastic-plastic one-storey frame structure is demonstrated in this section. The frame structure has a width L = 9.14 m, height h = 7.07 m and modulus of elasticity of 200 Gpa. The beam carries a total dead load of 3×10^3 N/m and columns are made of W8$\times$24 steel section. The initial stiffness of columns is computed as 1.17 $\times$ 10^5 N/m and damping ratio is taken to be 0.03. A sdof system is used to model the frame structure. The natural frequency of the elastic linear system was determined as 1.03 Hz. The spring yield strength in tension and compression is taken as 1.5×10^4 and -1.5×10^4 N, respectively. This, in turn, leads to defining yield displacement in tension and compression as 0.1285 and -0.1285 m, respectively.

4.2 Quantification of constraints

The frame structure is taken to be located at a site with firm soil condition and is subjected to uniform earthquake ground motion $\ddot{u}_g(t)$ at both support points. A set of 20 earthquake ground motions (N_r = 20) is used to quantify the constraints E, M_1, M_2 and M_3[6]. The selection of these records is based primarily on soil site conditions. This can be justified since earthquake accelerations measured on sites with similar soil conditions exhibit the same features (*e.g.* dominant soil frequency and Fourier spectrum). Thus, if the number of available ground motions at the given site is limited, records from other sites with similar geological soil conditions can be used. The question on the number of adequate records is difficult to be justified since the series representation (equation 5, page 4) does not converge as the number of records increases. However, it was observed in the numerical computations that $N_r \ge 10$ provides a smooth average Fourier spectrum for the site. Accordingly, it is hopped that this set of ground motions contains necessary characteristics of past records. Based on analysis of these records the following quantities are adopted; E = 4.17 m/sec$^{1.5}$, M_1 = 4.63 m/sec^2 (0.47 g), M_2 = 0.60 m/sec and M_3 = 0.15 m. The average dominant frequency of these records was observed to be around 1.65 Hz. The parameter β of the numerical integration algorithm is taken as 0.25, and, the time step Δt = 0.01 sec which was found to give satisfactory results in the numerical integration of the equation of motion. The convergence limits ℓ_1 and ℓ_2 were taken as 10^{-4} and 10^{-6}, respectively. The constrained nonlinear optimization problem is tackled by using the sequential quadratic optimization algorithm "*fmincon*" of the Matlab optimization toolbox[18]. As mentioned earlier, this algorithm requires the specification of an initial guess for the optimization variables a_i, i = *1, 2, …,*

N_r. In the numerical calculations, alternative initial starting solutions, within the visible region (which satisfy the imposed constraints), were examined and it was found that all guesses lead to the same optimal solution.

4.3 Dissipated energy

To gain more insights into nature of optimal earthquake loads computed it is of interest to quantify various forms of energy dissipated by the inelastic system. Several studies have utilized the energy dissipated by the structure in characterizing response analysis of dynamical systems[19,20]. Various energy terms can be quantified by integrating the structure equation of motion. Thus, the energy balance of the inelastic system is given as (see Equation (1))

Table 1 Constraint scenarios considered

Case	Constraints imposed
1	*E & PGA*
2	*E, PGA & PGV*
3	*E, PGA, PGV & PGD*

$$\int_0^u m\ddot{u}du + \int_0^u c\dot{u}du + \int_0^u f_s(u,\dot{u})du = -\int_0^u m\ddot{u}_g du \qquad (14)$$

The right side of the above equation represents the input energy to the structure since ground starts shaking until it comes to rest. The first energy term of the left side is the kinetic energy $E_K(t)$ of the mass associated with its motion relative to the ground and is given as

$$E_K(t) = \int_0^u m\ddot{u}(t)du = \int_0^{\dot{u}} m\ddot{u}(t)d\dot{u} = \frac{m[\dot{u}(t)]^2}{2} \qquad (15)$$

The second term of the left side indicates the energy dissipated by viscous damping $E_D(t)$ given by

$$E_D(t) = \int_0^u c\dot{u}(t)du = \int_0^t c[\dot{u}(t)]^2 dt \qquad (16)$$

The third term is the sum of the recoverable strain energy $E_S(t)$ and the energy dissipated by yielding $E_Y(t)$ and are given as

$$E_S(t) = \frac{f_s(t)}{2k};\ E_Y(t) = \int_0^u f_s(u,\dot{u})du - E_s(t) = \int_0^t \dot{u}(t) f_s(u,\dot{u})dt - E_s(t) \qquad (17)$$

In the present study, time-variations of energy terms given in Equations (15-17) are employed in quantifying and characterizing various forms of energy dissipated by the inelastic dynamical system.

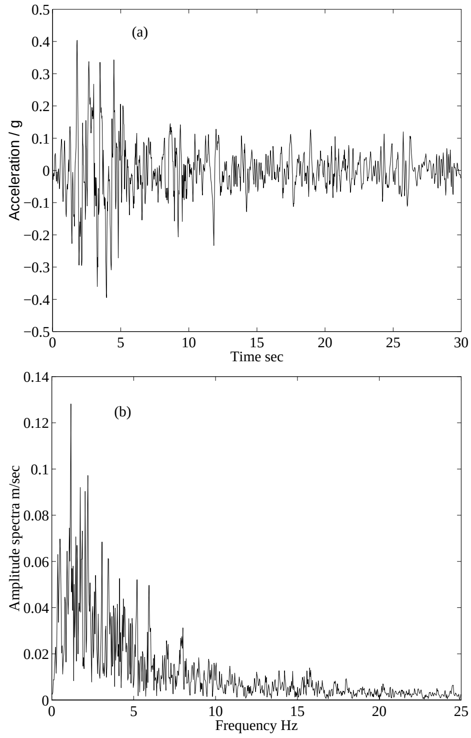

Figure 2. Critical $\ddot{u}_g(t)$ for inelastic structure, case (1) (a) Time history (b) Amplitude spectra

4.4 Results and discussions

To study the effect of alternative constraints imposed on critical earthquake excitations three constraint scenarios are examined (see Table 1). The numerical results obtained for the elastic-plastic structure are presented in figures (2) to (6) and tables 2-4. The critical earthquake load computed for constraint scenario case (1) is presented in figure (2). This figure shows the time history of the ground acceleration (figure 2(a)) and the Fourier amplitude spectra of $\ddot{u}_g(t)$ (figure 2(b)). The associated structure inelastic response is plotted in figure 3(a) and the hysteretic loops for the restoring force-displacement is shown in figure 3(b). Convergence of objective functions for inelastic and elastic structures are given in figure (4). The time-variations of different energy forms dissipated by the inelastic and elastic systems are provided in figure (5). To study the influence of the structure yield strength on critical earthquake loads and associated inelastic response a parametric study was carried out. The yield strength was varied, while

Table 2 Response of inelastic structure for different constraint scenarios

Case	1	2	3
μ_{max}	2.81	2.73	2.68
u_{max} (m)	-0.3602	-0.3507	-0.3443
u_p (m)	-0.0348	-0.0319	-0.0292

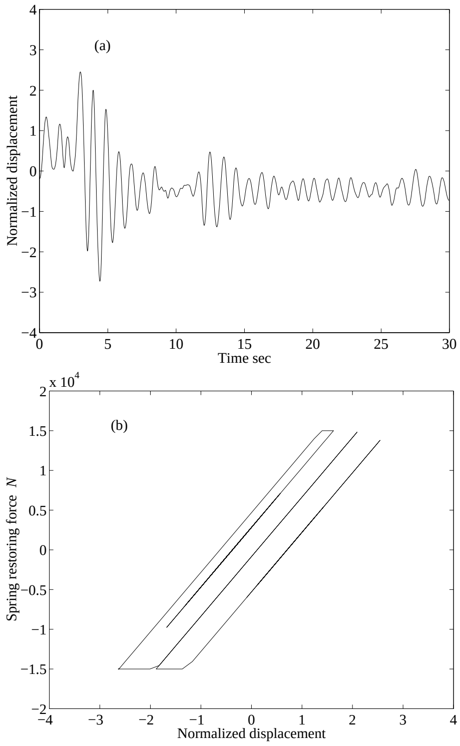

Figure 3. Response of elastic-plastic structure, case (1); (a) Displacement (b) Restoring force-displacement hysteretic loops

other parameters are kept unchanged, and the earthquake acceleration is computed for each value of yield strength. Figure (6) shows part of these results. A similar study to examine the effect of damping ratio on critical inputs for inelastic structures was also carried out. Results of this parametric study are presented in table 3. Based on studying these results the following observations are made:

1. It is observed that the critical ground acceleration for the elastic-plastic structure is rich in frequency content and possesses a peak amplitude at a frequency close to the natural frequency of the elastic system (see figures 2(a) and 2(b)). This peak, however, is seen to be significantly smaller than that observed in

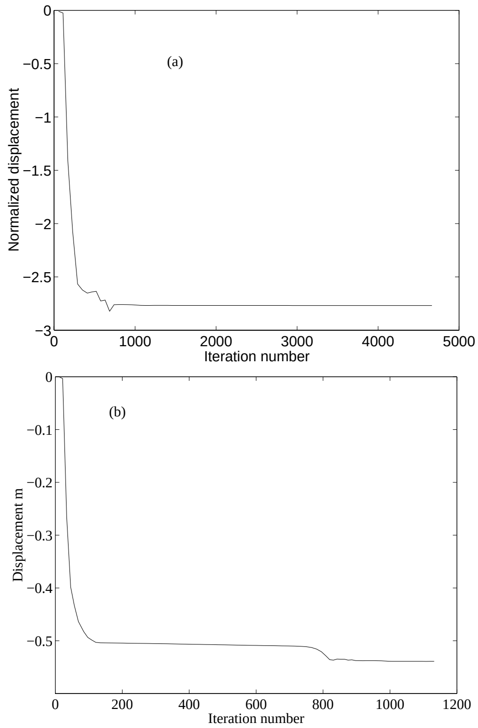

Figure 4. Convergence of objective function, case (1); (a) Inelastic structure (b) Elastic structure

critical $\ddot{u}_g(t)$ for the elastic structure. It emerges also that the Fourier spectrum of critical $\ddot{u}_g(t)$ has peak amplitude at the dominant frequency of past records (see figure 2(b)).

2. It is evident from the numerical results on critical ductility factor and associated inelastic displacement response that the time variation of the structure deformation differs from that of the elastic system (see figure 3(a)). Unlike the elastic system, inelastic system after it has yielded does not oscillate about its initial equilibrium position. Yielding causes the structure to drift from its initial equilibrium position and system oscillates around a new equilibrium position until this gets shifted by another yielding. Accordingly, after the ground stops shaking, the structure comes to rest at a position different from its initial equilibrium position. In other words, the structure permanent deformation remains after ground stops shaking. For instance, the permanent displacement response of the structure u_p was -0.0348 m. Additionally, the maximum value of

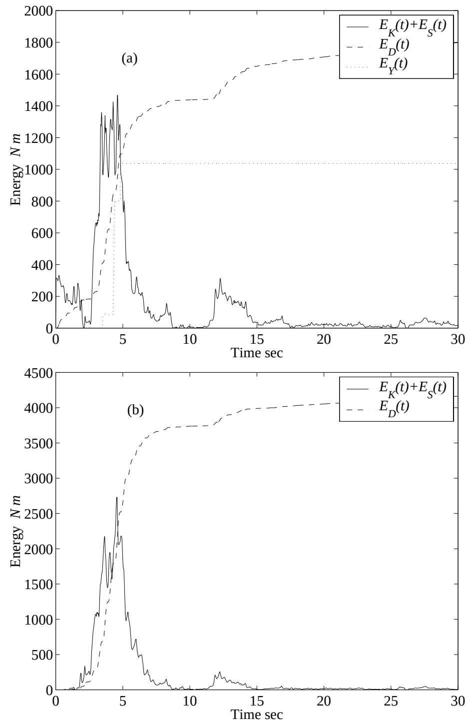

Figure 5. Dissipated energy, case (1) (a) Inelastic structure (b) Elastic structure

Table 3 Response of inelastic structure for different damping ratios, case (1)

Damping ratio	0.02	0.03	0.05
$\mu_{\max}$	3.25	2.81	2.36
u_{max} (m)	-0.4167	-0.3602	-0.3026
u_p (m)	-0.0493	-0.0348	-0.0215

the structure deformation and the point at which it occurs are different from those of the elastic system. Thus, the peak displacement response for the inelastic structure, case (1), is around -0.3602 m while the corresponding value for the elastic system was -0.5731 m. These peaks occur at t = 4.42 sec and t = 4.84 sec for the inelastic and elastic systems, respectively. The maximum value of the ductility factor was computed to be 2.81.

3. The convergence rate of the objective function with respect to the number of iterations of the optimization algorithm is seen to be faster for the elastic structure compared to that of the inelastic structure. While the objective function for the linear case reaches initial convergence to the optimal solution within about 800 iterations, the corresponding number of iterations when

Table 4 Sensitivity of objective function to constraint parameters, case (1)

Parameters	E	M_1	M_2	M_3
ε_1	0.22	0.06	0.04	0.02
ε_2	14.83	3.64	18.73	37.47

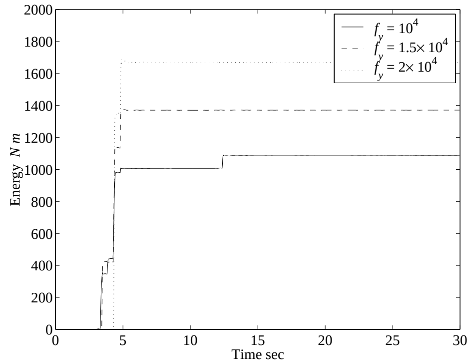

Figure 6. Energy dissipated by yielding, case (1)

inelastic behavior is considered is around 1000. The final convergence of the objective function for the elastic system is achieved within 1100 iterations, while for inelastic system the final convergence is achieved within 4800 iterations (see figure (4)). Furthermore, as might be expected, the computation CPU time necessary for the convergence of the objective function in the case of inelastic system is around three times that for the elastic system.

4. The inelastic structure dissipates energy, mainly, through yielding and viscous damping. This is evident since kinetic and recoverable strain energy terms diminish near the end of the ground shaking (see figure 5(a)). Viscous damping dissipates less energy from the inelastic system compared to that for the elastic system (see figures 5(a) and 5(b)). This is not surprising given that velocity response is higher for the elastic system. It is also obvious that the input energy to inelastic system differs from that for elastic system. Input energy to inelastic system, at point of maximum response, is significantly higher compared to other time points.

5. It is seen that the velocity and displacement constraints do not influence the derived critical earthquake inputs significantly. The effect of these constraints on the associated structural responses was also seen to be small (see Table 2). Accordingly, it can be concluded that energy and

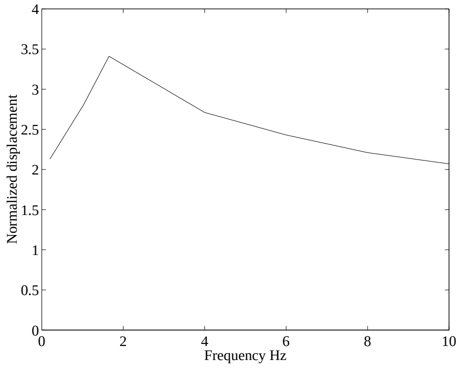

Figure 7. Variation of inelastic response with respect to natural frequency

acceleration constraints (case 1) are adequate to provide realistic earthquake loads.

6. The effect of the structure yield strength on the computed earthquake acceleration is seen to be significant. It is observed that for lower yield values the structure yields more frequently and for longer intervals. The structure dissipated energy, due to the inelastic behavior of the structure, is seen to be higher for higher yield strength (see Equation 17). Additionally, with higher yielding strength, the structure maximum response increases. Thus, the peak inelastic response associated with yield strength 10^4, 1.5×10^4 and 2×10^4 N were -0.2875, -0.3602 and -0. 4213 m, respectively. The associated ductility factors were 3.36, 2.81 and 2.46, respectively. The corresponding permanent deformation is -0.0221, -0.0348 and -0.0536 m, respectively.

7. The influence of damping ratio on the structure inelastic deformation was seen to be significant (see Table 3). As might be expected, for higher damping ratio the structure maximum inelastic response is seen to reduce. Thus, the structure maximum inelastic deformation was computed to be -0.4167, -0.3602 and -0.3026 for damping ratios 0.02, 0.03 and 0.05, respectively. The corresponding ductility factors were 3.25, 2.81 and 2.36, respectively. Similarly, the permanent deformation of the inelastic system reduces for higher values of damping ratio.

8. In order to study the sensitivity of critical response with respect to variations in values of constraints (E, M_1, M_2 and M_3), a limited amount of sensitivity analysis using numerical methods have been carried out. To study the sensitivity of critical response with respect to a specific parameter, the value of this parameter is changed by 1 per cent while other parameters are held fixed at their respective specified values. The optimization problem is re-solved with this change in place. This leads to the calculation of the percentage change in the critical response, denoted by ε_1, and also the ratio of change in the response value to the change in the parameter value, denoted by ε_2. These parameters provide an idea about the sensitivity of the objective function to the constraints. Table 4 summarizes the results of this calculation for constraint scenario (1). It evident from this table that the change in energy constraint alters the optimum solution considerably compared to similar changes in other parameters. Accordingly, it can be concluded that the optimum solution is more sensitive to the energy constraint compared to the constraints on peak values of acceleration, velocity and displacement.

Finally, with a view to investigate the effect of the natural frequency of the structure on the derived critical ground acceleration and associated structure inelastic response, an additional study is carried out. Herein, the structure natural frequency was varied (by varying the structure mass while other parameters are kept unchanged) and critical $\ddot{u}_g(t)$ is computed. These results are presented in figure (7). It follows from this figure that the natural frequency of the linear system significantly influences the critical acceleration and associated structure inelastic response. Structures having natural frequency close the dominant natural frequency of the site under consideration produce higher inelastic response compared to structures that have their natural frequency far from site dominant frequency.

5. CONCLUSIONS

The modeling of earthquake ground motion as design inputs for inelastic single-degree-of-freedom structures is studied. The earthquake load is modeled as a deterministic time history which is expressed as a linear combinations of past recorded ground motions. The coefficients of the series representation are computed such that the structure inelastic response normalized to yield displacement is maximized under a set of predefined constraints. These constraints are taken to reflect known characteristics of actual recorded ground motions at the site under consideration. Particularly, constraints on the total energy of the earthquake signal, and, bounds on peak values of ground acceleration, velocity and displacement are considered. The structure force-displacement relation is taken to possess an elastic-plastic behavior. The resulting nonlinear optimization problem is solved by using the sequential quadratic optimization method. It is shown that critical earthquake loads for the elastic-plastic structure differ from that for the same structure with linear behavior. Similarly, the time variation of the structure deformation differs from that of the elastic system. Unlike the elastic system, the inelastic system after it has yielded does not oscillate about its initial equilibrium position. Yielding causes the structure to drift from its initial equilibrium position and system oscillates around a new equilibrium position until this gets shifted by another yielding. The time-variation of alternative energy forms for the inelastic structure differ from those for the linear structure. Furthermore, it is seen that the inelastic structure dissipates the input energy, mainly, through yielding and damping. The present study, also, examined the influence of the structure yield strength and damping ratio on the derived earthquake load and associated structure response. It was found that for lower yield values the structure yields more frequently and for longer intervals. The effect of damping ratio was seen to be significant in reducing the structure inelastic deformation.

The proposed formulation was demonstrated with reference to the inelastic seismic response analysis of a frame structure modeled as a sdof system. Given the complexity of engineering structures, it is thus of significant interest to extend this formulation to mdof structures. It is also of significance to investigate the influence of treating nonlinear damping models in computing critical earthquake inputs for inelastic structures.

REFERENCES

1) PEER Center, Pacific Earthquake Engineering Research Center., http://peer.berkeley.edu, 2004.
2) Drenick, R.F.: Model-free design of aseismic structures, *Journal of Engineering Mechanics*, **96**, 483-493, 1970.
3) Shinozuka, M.: Maximum structural response to seismic excitations, *Journal of Engineering Mechanics*, **96**, 729-738, 1970.
4) Iyengar, R.N.: Matched inputs, Report 47, Series J., Center of Applied Stochastics, Purude University, West Lafayette, Ind, 1970.
5) Takewaki, I.: Seismic critical excitation method for robust design: A review, Journal of Structural Engineering, 128, 665-672, 2002.
6) Abbas A.M. and Manohar C.S.: Investigations into critical earthquake load models within deterministic and probabilistic frameworks, Earthquake Engineering and Structural Dynamics, 31, 813-832, 2002.
7) Abbas, A.M., Deterministic/Reliability-based critical earthquake load models for linear/nonlinear engineering structures, Ph. D. thesis, Department of Civil Engineering, Indian Institute of Science, 2002.
8) Iyengar, R.N.: Worst inputs and a bound on the highest peak statistics of a class of non-linear systems, Journal of Sound and Vibration, 25, 29-37, 1972.
9) Drenick, R.F.: The critical excitation of nonlinear systems, Journal of Applied Mechanics, 18, 333-336, 1977.
10) Philippacopoulos, A.J. and Wang, P.C.: Seismic inputs for nonlinear structures, Journal of Engineering Mechanics, 110, 828-836, 1984.
11) Westermo, B.D.: The critical excitation and response of simple dynamic systems, Journal of Sound and Vibration, 100, 233-242, 1985.
12) Pirasteh, A.A., Cherry, J.L. and Balling, J.A.: The use of optimization to construct critical accelerograms for given structures and sites, Earthquake Engineering and Structural Dynamics, 16, 597-613, 1988.
13) Takewaki, I.: Probabilistic critical excitation for MDOF elastic-plastic structures on compliant ground, Earthquake Engineering and Structural Dynamics, 30, 1345-1360, 2001.
14) Takewaki, I.: Critical excitation for elasr-plastic structures via equivalent linearization, Probabilistic Engineering Mechanics, 17, 73-84, 2002.
15) Abbas A.M., Manohar C.S.: Reliability-Based critical earthquake load models, II: Nonlinear structures, Journal of Sound and Vibration, in press, 2005.
16) Chopra, A.K., Dynamics of structures, Second Edition, Prentice-Hall, New Jersey, 2001.
17) Arora, J.S., Introduction to optimum design, Elsevier Academic Press, San Diego, 2004.
18) Caleman, T., Branch, M.A. and Grace, A., Optimization toolbox for the use with Matlab, user's guide version 2(Release 11), The MATH WORKS Inc., 1999.
19) Uang, C.M., Bereto, V.V.: Evaluation of seismic energy in structures, Earthquake Engineering and Structural Dynamics, 19, 77-90, 1999.
20) Takewaki, I.: Bound of earthquake input energy, Journal of Structural Engineering, 130, 1289-1297, 2004.

(**Received March 15, 2005**)